

The Inverse Dynamics of Cassino Parallel Manipulator

JOÃO CARLOS MENDES CARVALHO (*), MARCO CECCARELLI (#)

(*) *Universidade Federal de Uberlândia*
Faculdade de Engenharia Mecânica, 38400-902 Uberlândia – MG, Brazil
e-mail: jcmendes@mecanica.ufu.br

(#) *Università di Cassino*
Dipartimento di Meccanica, Strutture, Ambiente e Territorio, Laboratorio di Robotica e Meccatronica,
Via di Biasio 43, 03043 Cassino (FR), Italy
e-mail: ceccarelli@ing.unicas.it

Abstract. In this paper we have presented an analytical model for the dynamics of Cassino Parallel Manipulator – CaPaMan. In order to compute the input torques, which are necessary for a given trajectory of movable platform, the dynamic effects of the movable platform have been superposed to the dynamic effects of articulated parallelograms of the leg design. The dynamic behaviour of movable platform has been analysed by means of Newton-Euler equations and the behaviour of articulated parallelograms has been formulated using the kinetostatic analysis of mechanisms. Results of numerical simulations have been presented to show the feasibility of the proposed approach and performance of CaPaMan..

Keywords: Robot Dynamics, Parallel Manipulators, Numerical Simulation.

1. Introduction

Parallel architectures have been extensively studied since they can be used in several applications such as manipulation, packing, assembly and disassembly processes, motion simulation and milling machines. The interest can be justified because they show better rigidity, accuracy positioning and payload capacity with respect to the serial structures and can operate at higher velocities and accelerations. Thus, great attention has been addressed from theoretical and practical viewpoint with several new parallel mechanisms that have been conceived and designed in the recent years such as presented in Clavel [1] Merlet and Gosselin [2] and Jacquet et al. [3]. A new parallel manipulator named as Cassino Parallel Manipulator - CaPaMan, having three degrees of freedom, was conceived at the Laboratory of Robotics and Mechatronics in Cassino, Italy. Researches have been carried out with the aim to develop a parallel mechanism which can be easily built and operated. Performances and suitable formulation for kinematics have been investigated and are reported in Ceccarelli [4] and [5]; Ceccarelli and Figliolini [6], Carvalho and Ceccarelli [7], including an application of CaPaMan as an

earthquake simulator, which can reproduce a really happened earthquake [8] and [9]. Some experimental validations are reported in Ceccarelli et al. [9].

Since in fast robotic operations the inertial effects are important and cannot be neglected, the robot dynamic behaviour must be known to improve the accuracy and control of the robot motion.

In this paper an analytical formulation for the inverse dynamics of CaPaMan is proposed. The symmetry characteristics of CaPaMan structure have been useful to formulate the inverse dynamics by considering the inertia of the movable platform and the three 4-bar leg mechanisms, to compute the input torques which are necessary for a given trajectory of movable platform. Results of a numerical simulation are reported for a specific trajectory as an illustrative example.

2. CaPaMan Architecture and Kinematics

CaPaMan - Cassino Parallel Manipulator is a 3 d.o.f. parallel manipulator, which is characterized by three 4-bar mechanism legs AP assembled in an equilateral triangle way with respect to the fixed base FP as shown in Fig. 1. On the coupler link of each 4-bar mechanism is installed a prismatic joint SJ that is connected to the movable platform MP by a rod CB and a spherical joint BJ. Thus the rod CB may translate along the prismatic guide SJ keeping its vertical posture while the spherical joint BJ allows the movable platform to rotate in the space. In this paper all the three 4-bar mechanism legs have been considered as articulated parallelograms. The kinematic variables are the input crank angles α_k ($k=1,2,3$) of the articulate parallelograms and s_k is the coordinate displacement of the passive prismatic joint.

A frame $O_k X_k Y_k Z_k$ has been assumed fixed on the plane of each k articulated parallelogram with O_k coinciding with the center point of frame link a_k . The base frame $OXYZ$ has been located in the center of the fixed plate FP and a frame $HX_p Y_p Z_p$ has been fixed to the movable platform MP where the origin H is the center of MP.

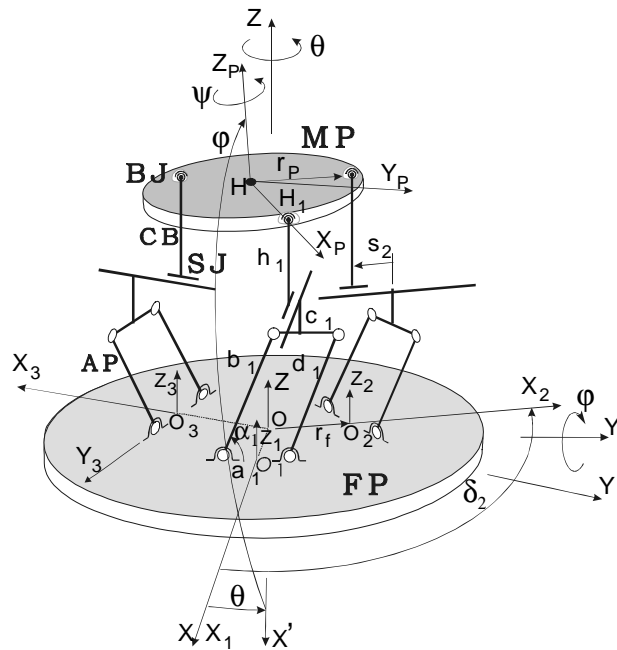


Fig. 1. Architecture and kinematic parameters of CaPaMan.

By using a suitable analysis procedure with a vector and matrix formulation, the position coordinates x , y and z of the center point H and the orientation angles θ , φ and ψ of the movable platform MP can be expressed as function of the coordinates y_k and z_k of the articulation points H_k , which are expressed with respect to the frame $O_kX_kY_kZ_k$ fixed on mechanism leg. These coordinates can be easily expressed as function of the AP input angles α_k ($k=1,2,3$).

Thus, the direct displacement analysis can be formulated to give the expressions of position of the center point H and orientation of movable platform as a function of coordinates y_k and z_k ($k=1,2,3$) in the form [4]

$$\begin{aligned} x &= \frac{y_3 - y_2}{\sqrt{3}} - \frac{r_p}{2} (1 - \sin\varphi) \cos(\psi - \theta); & y &= y_1 - r_p (\sin\psi \cos\theta + \cos\psi \sin\varphi \sin\theta) \\ z &= \frac{z_1 + z_2 + z_3}{3}; & \theta &= \sin^{-1} \left[2 \frac{y_1 + y_2 + y_3}{3r_p (1 + \sin\varphi)} \right] - \psi; & \psi &= \tan^{-1} \left(\sqrt{3} \frac{z_3 - z_2}{2z_1 - z_2 - z_3} \right) \\ \varphi &= \cos^{-1} \left(\pm \frac{2}{3r_p} \sqrt{z_1^2 + z_2^2 + z_3^2 - z_1z_2 - z_2z_3 - z_1z_3} \right) \end{aligned} \quad (1)$$

with ($z \geq z_1 \Rightarrow$ " + "; $z < z_1 \Rightarrow$ " - ")

The input motion of the input crank b_k can be given by a cubic function of time t between given initial α_{ki} and final α_{kf} angles at initial t_{ki} and final t_{kf} times, respectively, as

$$\alpha_k = \alpha_{ki} + \frac{3(\alpha_{kf} - \alpha_{ki})}{(t_{kf} - t_{ki})^2} t^2 - \frac{2(\alpha_{kf} - \alpha_{ki})}{(t_{kf} - t_{ki})^3} t^3 \quad (2)$$

since a PID control of the actuators is available for commercial motors.

Analysis of workspace, orientation capabilities and displacement generation for CaPaMan are presented and discussed in Ceccarelli [4] and Ceccarelli and Figliolini [6].

3. CaPaMan Dynamics

The analytical model for dynamics of CaPaMan has been formulated to compute the input torques which are necessary for a given trajectory of movable platform. In order to simplify the mathematical model the effects of link elasticity and viscous damping of the joints have been neglected. Linkages are assumed to be composed of rigid bodies connected by frictionless joints without clearance in joints. Position, velocity and acceleration of the movable platform and links of articulated parallelograms are given by the direct kinematics.

3.1. Dynamics of Movable Platform

The peculiar kinematic formulation and symmetry properties of CaPaMan architecture can be useful to analyse its dynamic behaviour by means of Newton-Euler equations. The dynamic equilibrium for the mobile platform can be expressed as

$$F + F_{ext} + G = m a_H \quad \text{and} \quad N + N_{ext} = I\dot{\omega} + \omega \times (I\omega) \quad (3)$$

with

$$F = \sum_{k=1}^3 F_k \quad \text{and} \quad N = \sum_{k=1}^3 (r_p R u_{kp}) \times F_k \quad (k=1,2,3) \quad (4)$$

Where F_{ext} and N_{ext} are the external force and torque; F is the sum of the reaction force F_k ($k=1,2,3$) acting at point H_k of MP and N is the consequent torque; G is the platform weight as shown in Figure 3. m is the mass of the platform; a_H is the acceleration of center point H; $\dot{\omega}$ and ω are the angular acceleration and velocity of the movable plate. The inertia matrix I of the movable plate can be determined as $I = R I_c R^T$, by using the rotation matrix R between the $OXYZ$ and $HX_p Y_p Z_p$ reference frames, and the inertia matrix I_c of MP with respect to its center of mass.

By neglecting the friction in the prismatic joints SJ, the only forces applied to the articulated points H_k by rods CB are those which are contained in the plane of the articulated parallelogram i.e. F_{ky} and F_{kz} ($k=1,2,3$) as shown in Fig. 2. Thus, the components of the resultant force F and torque N , given by Eqs. (4), can be written as

$$\begin{Bmatrix} F_x \\ F_y \\ F_z \\ N_x \\ N_y \\ N_z \end{Bmatrix} = \begin{Bmatrix} -\frac{\sqrt{3}}{2} F_{2y} + \frac{\sqrt{3}}{2} F_{3y} \\ F_{1y} - \frac{1}{2} F_{2y} - \frac{1}{2} F_{3y} \\ F_{1z} + F_{2z} + F_{3z} \\ -u_{1z} F_{1y} + \frac{1}{2} u_{2z} F_{2y} + \frac{1}{2} u_{3z} F_{3y} + u_{1y} F_{1z} + u_{2y} F_{2z} + u_{3y} F_{3z} \\ -\frac{\sqrt{3}}{2} u_{2z} F_{2y} + \frac{\sqrt{3}}{2} u_{3z} F_{3y} - u_{1x} F_{1z} - u_{2x} F_{2z} - u_{3x} F_{3z} \\ \frac{1}{2} (\sqrt{3} u_{2y} - u_{2x}) F_{2y} - \frac{1}{2} (\sqrt{3} u_{3y} + u_{3x}) F_{3y} + u_{1x} F_{1y} \end{Bmatrix} \quad (5)$$

with

$$\begin{Bmatrix} u_{kx} \\ u_{ky} \\ u_{kz} \end{Bmatrix} = r_p R \begin{Bmatrix} \cos \delta_k \\ \sin \delta_k \\ 0 \end{Bmatrix}; \quad (k=1,2,3) \quad \text{and} \quad \delta_1 = 0; \delta_2 = 2\pi/3; \delta_3 = 4\pi/3. \quad (6)$$

Thus, equations (3), (4), (5) and (6) can be solved in a closed form to obtain an explicit expression for forces F_{ky} and F_{kz} .

Once the reaction forces in the spherical joints H_k are computed, the torque τ_{pk} ($k=1,2,3$) on the input crank shaft of each articulated parallelogram can be obtained as

$$\tau_{pk} = F_{kz} \left(b_k \cos \alpha_k + \frac{c_k}{2} \right) - F_{ky} (b_k \sin \alpha_k + h_k) \quad , \quad (k=1,2,3) \quad (7)$$

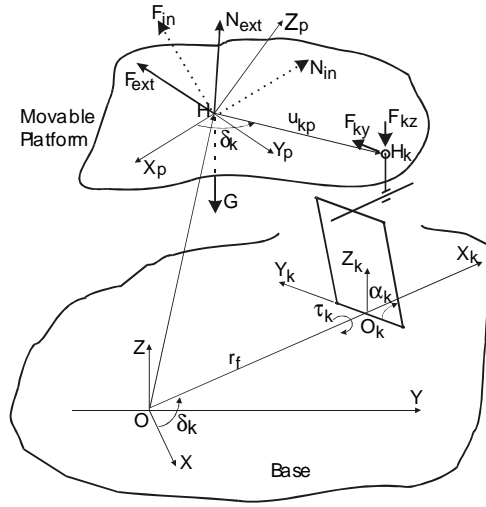


Fig. 2. Forces acting on the movable platform and the spherical joints.

3.2. Dynamics of Articulated Parallelograms

For the following analysis one can assume that the linear accelerations of the mass centers and the angular accelerations of the moving links have been determined by the kinematic analysis of the articulated parallelograms; the mass of links b_k and d_k are smaller than the platform and therefore negligible; the mass centers of links are coinciding with the figure centers.

By using a kinetostatic analysis of mechanisms the dynamic equilibrium in the presence of the three inertia forces F_{inbk} , F_{inck} and F_{indk} , whose application points are determined by offset e_{bk} , e_{ck} and e_{dk} from the mass center of links b , c and d , respectively, as shown in Fig.3, are given as

$$\vec{F}_{inbk} = -m_{bk} \vec{a}_{Gbk}; \quad \vec{F}_{inck} = -m_{ck} \vec{a}_{Gck}; \quad \vec{F}_{indk} = -m_{dk} \vec{a}_{Gdk} \quad (8)$$

$$e_{bk} = \frac{I_{Gbk} \dot{\omega}_{bk}}{F_{inbk}} = \frac{I_{Gbk} \ddot{\alpha}_k}{F_{inbk}}; \quad e_{ck} = \frac{I_{Gck} \dot{\omega}_{ck}}{F_{inck}} = 0; \quad e_{dk} = \frac{I_{Gdk} \dot{\omega}_{dk}}{F_{indk}} = \frac{I_{Gdk} \ddot{\alpha}_k}{F_{indk}} \quad (9)$$

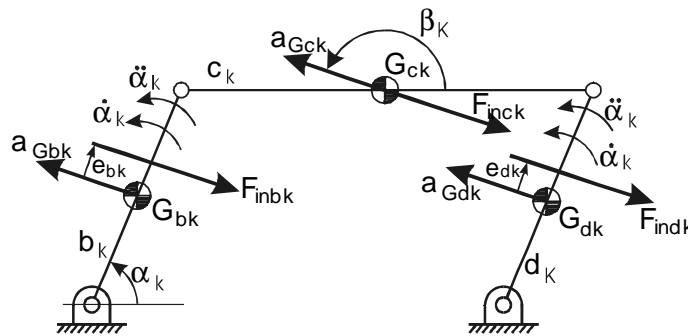


Fig. 3. Inertia forces arising in the articulated parallelogram k ($k=1,2,3$).

Using the principle of superposition, the effects of each inertia force of links can be treated separately and then superposed to determine their combined effect. The input torque τ_{Mk} is obtained from the total effect of the inertia of the three moving links and link c mass m_{ck} as the sum of the torques that are obtained from each inertia force and link c mass. Thus, the input torque τ_{Mk} can be written as

$$\tau_{Mk} = 2l_{bk} F_{inbk} \sin(\alpha_k - \beta_k - \pi) + F_{23k} b \sin(\alpha_k + \pi - \gamma_k) + (b^* \cos \alpha_k + c/2) m_{ck} g \quad (10)$$

With

$$l_{bk} = \frac{b}{2} + \frac{I_{Gbk} \ddot{\alpha}_k}{F_{inbk}} \frac{1}{\sin(\alpha_k - \beta_k + \pi)}$$

$$F_{23k} = \sqrt{\left\{ F_{inck} \left[\cos(\beta_k + \pi) + \frac{\sin(\pi - \beta_k)}{2 \tan \alpha_k} \right] \right\}^2 + \left[\frac{F_{inck} \sin(\beta_k + \pi)}{2} \right]^2}$$

$$\gamma_k = tg^{-1} \left\{ \frac{F_{inck} \left[\cos(\beta_k + \pi) + \frac{\sin(\pi - \beta_k)}{2 \tan \alpha_k} \right]}{\left[\frac{F_{inck} \sin(\beta_k + \pi)}{2} \right]} \right\} \quad (11)$$

in which the angle β_k defines the direction of the acceleration of the mass center of the link k with respect to the horizontal axis, assumed to be positive counter-clockwise. Similarly, γ_k defines the direction of the reaction force vector acting on the ground pivot of link d_k .

3.3. The Total Input Torque

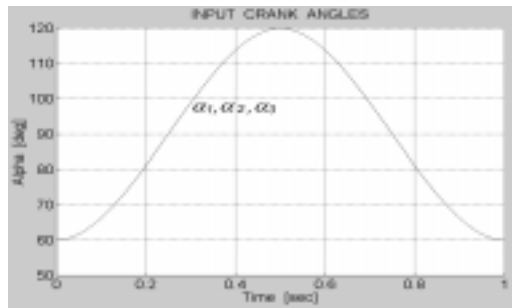
Since the derived equations are algebraic and linear in the inertia forces, the principle of superposition can be applied. Thus the dynamic effects of movable platform can be superposed to the dynamics effects of articulated parallelograms.

The total torque τ_k on the input crank shaft of each articulated parallelogram can be obtained by summing the torques τ_{Pk} and τ_{Mk} that are obtained by the analysis of dynamics of the movable platform and the articulated parallelograms, respectively.

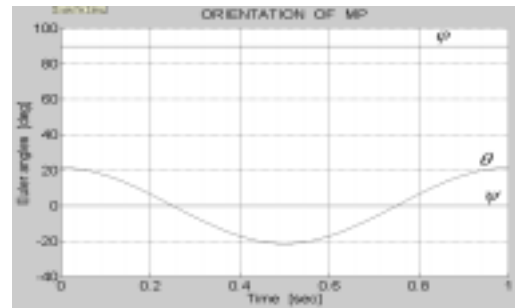
4. Numerical Simulations

Several numerical simulations have been carried out and experimental activities are still undergoing to validate the proposed formulation and verify the dynamic behaviour of CaPaMan. The first experiments have given satisfactory agreement for accelerations and torques, as shown in [8] and [10].

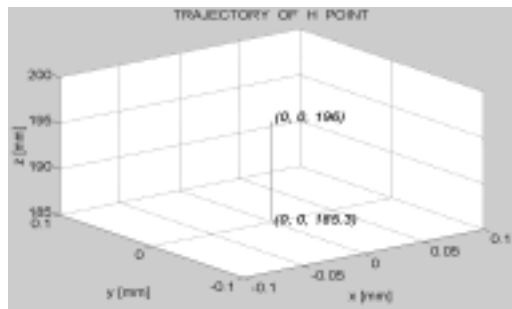
In this section we have been presented an illustrative example of a numerical simulation by considering the movable platform to move along a vertical straight line and assuming that no external force and torque are applied to the movable platform, i.e. $F_{ext}=0$ and $N_{ext}=0$, Fig. 4. The vertical motion is obtained when the three input crank angles α_k are equals. A cycle is simulated considering that the



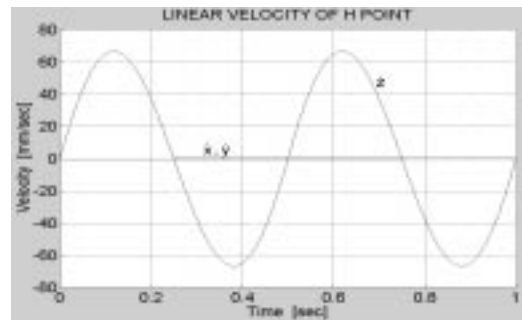
(a)



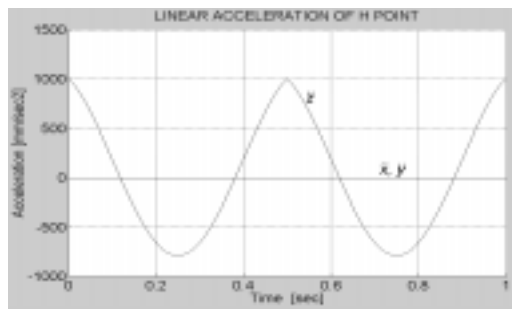
(b)



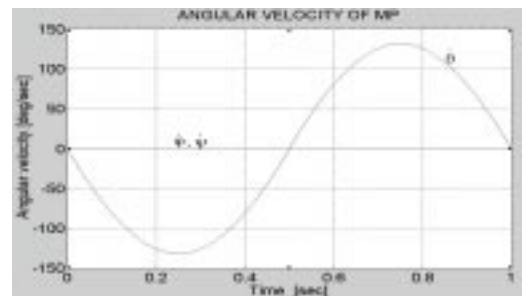
(c)



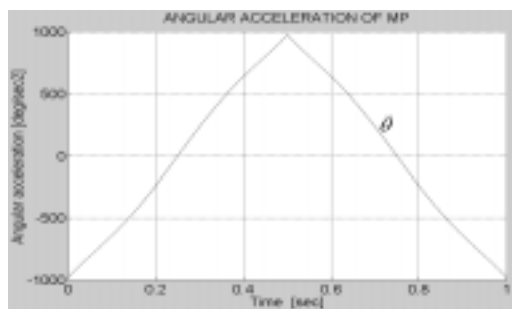
(d)



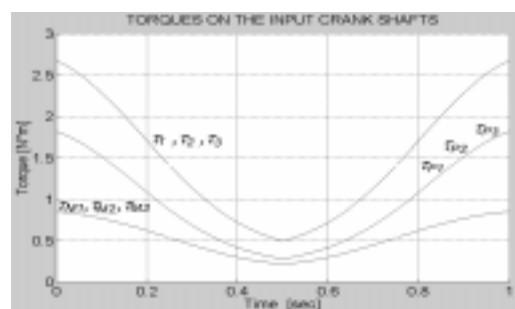
(e)



(f)



(g)



(h)

Fig. 4. Numerical results of a dynamic simulation of CaPaMan for a vertical straight line motion.

crank starts at the initial input angles $\alpha_{ki}=60\text{deg}$, stops at the final angles $\alpha_{kf}=120\text{deg}$ and goes back to the start angles $\alpha_{ki}=60\text{deg}$ in 1 sec, as shown in Figure 4a. This means that H point describes two linear movements starting at point (0, 0, 185.3)mm to the point (0, 0, 196)mm, and back to the start point as shown in Fig. 4c. The vertical velocity and acceleration are shown in Figs. 4d and 4e, respectively. The linear vertical motion is accomplished with a rotation θ about the axis Z as shown in Fig. 4b, with its velocity and acceleration shown in Figs. 4f and 4g, respectively. Figure 4h shows the history of torques at the input crank shafts. Figure 4h gives also the torques from the effects of the articulated parallelogram motion τ_{Mk} , the movable platform motion τ_{pk} and the total torque τ_k . Since the motion of the three articulated parallelograms is the same the input torques are equals. The reported simulation refers to the specific dimensions of the built prototype at the Laboratory of Robotics and Mechatronics of Cassino, which has the following data: $b_k=80\text{mm}$; $h_k=116\text{mm}$; $c_k=200\text{mm}$; $r_p=r_b=109.5\text{mm}$; $m=2.912\text{kg}$; $m_{dk}=m_{bk}=0.103\text{kg}$; $m_{ck}=0.547\text{kg}$; $I_{Gck}=0.0027\text{kgm}^2$; and $I_{Gbk}=I_{Gdk}=0.00013\text{kgm}^2$, ($k=1,2,3$).

6. Conclusion

An analytical model has been formulated for the inverse dynamics of CaPaMan – Cassino Parallel Manipulator. The peculiar kinematics and symmetry properties of CaPaMan has been useful to analyse the dynamic behaviour of the movable platform using Newton-Euler equations and the kinetostatic analysis of mechanisms for the analysis of the three articulated parallelogram legs.

References

- [1] Clavel, R., 1988, DELTA: A Fast Robot with Parallel Geometry, Proc. 18th Int. Symp. on Industrial Robots, Lausanne, pp.91-100.
- [2] Merlet, J.P., Gosselin, C., 1991, Nouvelle Architecture Pour Manipulateur Parallèle a Six Degrés de Liberté, Mechanism and Machine Theory, Vol.26, No.1, pp.77-90.
- [3] Jacquet, P., Danescu, G., Carvalho, J.C.M., Dahan, M., 1992, "A spatial fully parallel manipulator", in Proceedings of *World Congress on the Theory of Machines and Mechanisms*, Udine.
- [4] Ceccarelli, M., 1997, A New 3 dof Spatial Parallel Mechanism, Mechanism and Machine Theory Vol.32, No.8, pp. 895-902.
- [5] Ceccarelli, M., 1998, A Stiffness Analysis for CaPaMan (Cassino Parallel Manipulator), Conference on New Machine Concepts of Handling and Manufacturing Devices on the Basis of Parallel Structures, VDI 1427, Braunschwig, pp.67-80.
- [6] Ceccarelli, M., Figliolini, G., 1997, Mechanical Characteristics of CaPaMan (Cassino Parallel Manipulator), 3rd Asian Conference on Robotics and its Application, Tokyo, Japan, pp.301-308.
- [7] Carvalho, J.C.M., Ceccarelli, M., 1999a, A Dynamic Analysis for Cassino Parallel Manipulator, 10th World Congress on Theory of Machines and Mechanisms / IFToMM'99, Oulu, pp.1202-1207.
- [8] Ceccarelli, M., Pugliese, F., Lanni, C., Carvalho, J.C.M., 1999a, CaPaMan (Cassino Parallel Manipulator) as Sensored Earthquake Simulator, IEEE/RSJ - International Conference on Intelligent Robots and Systems, Kyongju, pp.1501-1506.
- [9] Carvalho, J.C.M., Ceccarelli, M., 1999b, Seismic Motion Simulation Based on Cassino parallel Manipulator, 15th Brazilian Congress on Mechanical Engineering / COBEM'99, Águas de Lindóia.
- [10] Ceccarelli, M., Pugliese, F., Carvalho, J.C.M., 1999b, An Experimental System for Measuring CaPaMan Characteristics, 8th International Workshop on Robotics in Alpe-Adria-Danube Region / RAAD'99, Munich.